Chapter 1

Introduction

Chapter 2

Theory

2.1 Richard's Equation

The water flow in porous media can be described with the formula of Richard. The equation is here derived. The water flux density vector, $\mathbf{q}$ can be calculated by the Darcy´s law. For a two-dimensional vertical transect it yields:

$$\mathbf{q} = -\mathbf{K}(\psi)\nabla(\psi + z) \tag{2.1}$$

where $\mathbf{K}(\psi)$ is the hydraulic conductivity tensor, ψ is the potential head. The x-axis is chosen in horizontal direction and the z-axis is positive upwards. The conductivity tensor can be expressed as:

$$\mathbf{K} = \begin{bmatrix} K_{xx} & K_{xz} \\ K_{zx} & K_{zz} \end{bmatrix} \tag{2.2}$$

For the model with rectangular cells we have chosen that the principal directions of the anisotropic medium are parallel with the x- and z-axis, i.e.

$$\mathbf{K} = \begin{bmatrix} K_{xx} & 0 \\ 0 & K_{zz} \end{bmatrix} \tag{2.3}$$

The mass balance for the system gives

$$\frac{\partial \theta}{\partial t} = -\nabla \cdot \mathbf{q} - \Gamma \tag{2.4}$$

where θ is the water content and Γ is the sink term. The partial differential equation can be developed by combining Darcy´s law, equation 2.1 and the mass balance, equation 2.4, thus

$$\frac{\partial \theta}{\partial t} = \nabla \cdot (\mathbf{K}(\psi)\nabla(\psi + z)) - \Gamma \tag{2.5}$$

This is known as Richard's equation. For the modeling is assumed that the soil-water retention is without hysteresis, i.e. there is a unique relation between the matric pressure potential and the water content.

To solve Richard's equation it is necessary to specify initial and boundary conditions. The boundary conditions specify a combination of ψ and its derivative on the boundary. In the prototype it is possible to use different forms of flux (Neumann) and predescribed pressure (Dirichlet) boundary conditions. The problem to be solved for determining the water movement can be summarized to

$$\begin{aligned} &\frac{\partial \theta}{\partial t} = \nabla \cdot (\mathbf{K}(\psi)\nabla(\psi + z)) - \Gamma \text{ in } \Omega \\ &\bar{\mathbf{n}} \cdot (\mathbf{K}(\psi)\nabla(\psi + z)) = -q \text{ on } \partial\Omega^N \\ &\psi = \psi_0 \text{ on } \partial\Omega^D \end{aligned} \tag{2.6}$$

where $\bar{\mathbf{n}}$ is the outward unit normal, and q is the size of the size of the outward flow from the domain. ψ_0 is the predescribed pressure at the boundary. $\partial\Omega^N$ and $\partial\Omega^D$ are part of the boundary with Neumann and Dirichlet boundaries, respectively such that $\partial\Omega = \partial\Omega^N \cup \partial\Omega^D$. Each of $\partial\Omega^N$ and $\partial\Omega^D$ are not necessarily one continuous curve piece. For lower boundary condition is a special case of the Neumann boundary conditions often applied. It here assumed that the flow it is only driven by the gravity (gravity boundary condition), i.e. $\partial\psi/\partial x = \partial\psi/\partial z = 0$ which gives

$$q = \bar{\mathbf{n}} \cdot \begin{bmatrix} 0 \\ K_{zz} \end{bmatrix} \tag{2.7}$$

Another often used boundary condition is the seepage boundary condition where we for $\psi > 0$ have specified pressure corresponding to the depth of the overlaying water. For $\psi \leq 0$ have specified flow to be equal to 0, i.e. a Dirichlet boundary condition for $\psi > 0$ and a Neumann boundary condition for $\psi \leq 0$.

Chapter 3

2 Dimensional Model

3.1 Finite Volume Method

3.1.1 Mesh

In Daisy2D, the domain, Ω is divided into N non-overlapping polygons, also denoted control volumes or cells. In Daisy2D it should be possible to choose between grids consisting of only rectangular cells or meshes consisting of trapezoids with two vertical faces. Figure 3.1 shows a grid only consisting of rectangular cells. The domain Ω in the figure is in divided into 3 subdomains, each consisting of a whole number of cells. Each subdomain can contain different soils with different hydraulic properties. The grid shown in figure 3.2 consists of trapezoids (where most of them also are rectangles). Only in the proximity of the drainpipe (see figure 3.3), the cells are not rectangular.

The quadrilateral (rectangular or trapezoid) cells are denoted Q_i where $i = 1, 2, \cdots, N$. $|Q_i|$ denotes the area of Q_i, and ∂Q_i is the boundary of Q_i i.e. the edges (or faces) of Q_i. All internal edges e_{ij} are labeled by indices, i and j of the adjacent cells that shares face. The grid is constructed such that only whole faces are shared ($e_{ij} = Q_i \cap Q_j$). The length of e_{ij} is $|e_{ij}|$ and the unit normal vector pointing from $Q_i$into Q_j and orthogonal to e_{ij} is denoted $\bar{\mathbf{n}}_{ij}$.

σ_i contains cell indices of cells sharing faces with cell i. σ_i' contain indices of cell faces of cell i witch are are placed on $\partial\Omega$, i.e. it is not shared with another cell. σ_i' is into two subsets, $\sigma_i'^D$ and $\sigma_i'^N$ of boundary cell faces with a Dirichlet and Neumann boundary condition, respectively.

3.1.2 Cell mass-balances

Richards equation is integrated over control volume (here a cell), Q_i. By applying the divergence theorem by Green-Gauss, we obtain

$$\int_{Q_i} \frac{\partial \theta}{\partial t} d\Omega = \int_{\partial Q_i} (\mathbf{K}(\psi)\nabla(\psi + z)) \cdot \bar{\mathbf{n}} dl - \int_{Q_i} \Gamma d\Omega \tag{3.1}$$

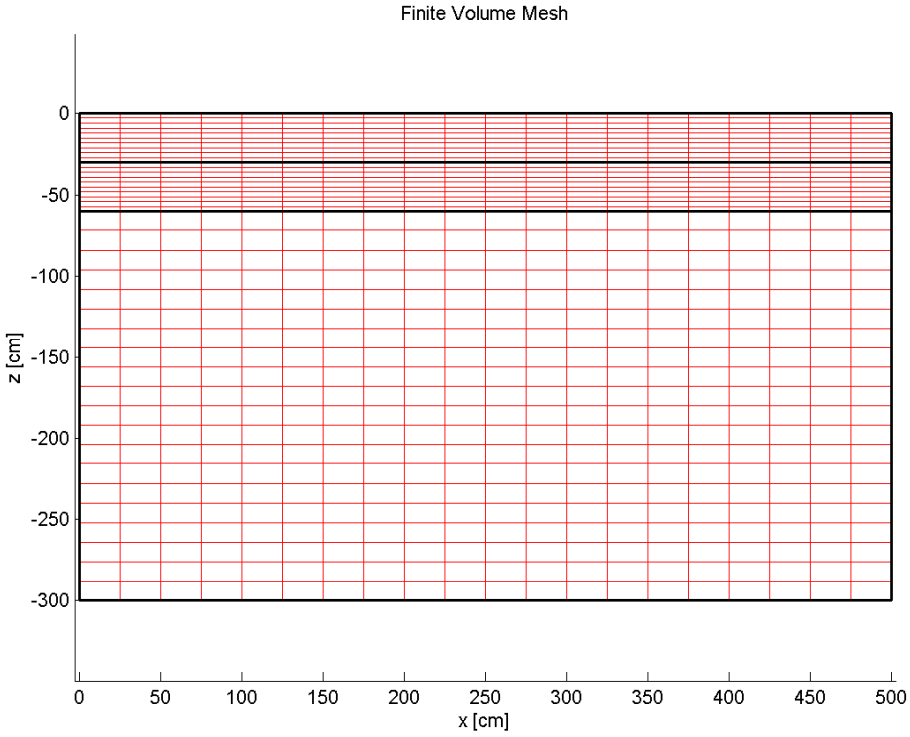

Figure 3.1: Example of grid consisting of rectangular cells.

where $\bar{\mathbf{n}}$ is the outwarded unit normal and ∂Q_i the boundary of Q_i. The cell averages of θ and ψ are denoted θ_i and ψ_i. θ_i and ψ_i, $i = 1, 2, \cdots N$ where N is the number of cells are collected in the vectors $\boldsymbol{\theta}$ and $\boldsymbol{\psi}$. Discretising equation 3.1 on a grid consisting of quadrilaterals yield

$$|Q_i|\frac{d\theta_i}{dt} = \sum_{j\in\sigma_i} D_{ij}(\boldsymbol{\psi}) + \sum_{j\in\sigma_i} G_{ij}(\boldsymbol{\psi}) + \sum_{j'\in\sigma_i'} B_{ij'}(\boldsymbol{\psi}) - S_i(\boldsymbol{\psi}) \qquad (3.2)$$

where:

- $D_{ij}(\boldsymbol{\psi})$ describe the diffusive transport between internal borders
- $G_{ij}(\boldsymbol{\psi})$ describe the gravitational transport between internal boundaries
- $B_{ij'}(\boldsymbol{\psi})$ describe flux for external boundaries $j' \in \sigma_i'$
- $S_i(\boldsymbol{\psi})$ is the source term (point and area distributed sources) in the cell.

The diffusive transport from cell i to cell j can be calculated as

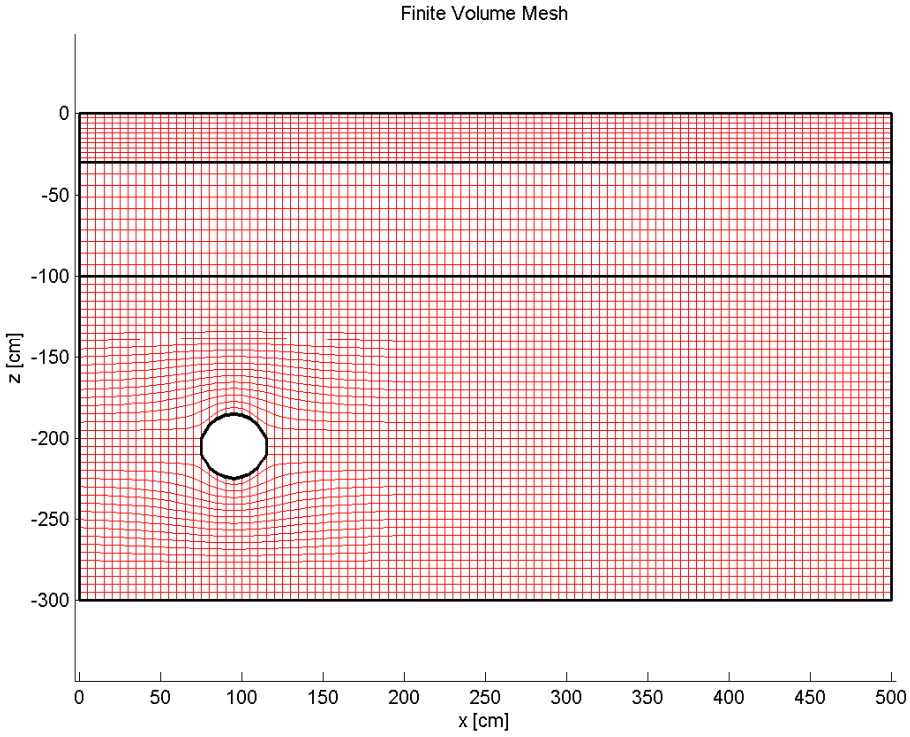

Figure 3.2: Example of grid consisting of trapezoids.

$$D_{ij}(\boldsymbol{\psi}) = |e_{ij}|(\mathbf{K}(\boldsymbol{\psi}) \cdot (\nabla\psi)_{ij}) \cdot \bar{\mathbf{n}}_{ij} \tag{3.3}$$

For evaluating equation 3.3 it is necessary to estimate the gradient $(\nabla\psi)_{ij}$. $(\nabla\psi)_{ij}$ is evaluated a different method for meshes with rectangular cells than for the more generel and complicated situation with meshes consisting of trapezoid cells. The gravitational transport from cell i to cell j can be calculated as

$$G_{ij}(\boldsymbol{\psi}) = |e_{ij}|(\mathbf{K}(\boldsymbol{\psi}) \cdot ([0\ 1]^T)) \cdot \bar{\mathbf{n}}_{ij} \tag{3.4}$$

The boundary flux term is split into the contribution from boundaries with Neumann and Dirichlet condition respectively:

$$\sum_{j' \in \sigma_i'} B_{ij'}(\boldsymbol{\psi}) = \sum_{j' \in \sigma_i'^N} B^N_{ij'}(\boldsymbol{\psi}) + \sum_{j' \in \sigma_i'^D} B^D_{ij'}(\boldsymbol{\psi}) \tag{3.5}$$

For the boundaries with Neumann conditions we have

$$B^N_{ij'}(\boldsymbol{\psi}) = -q_{ij'}|e_{ij'}| \tag{3.6}$$

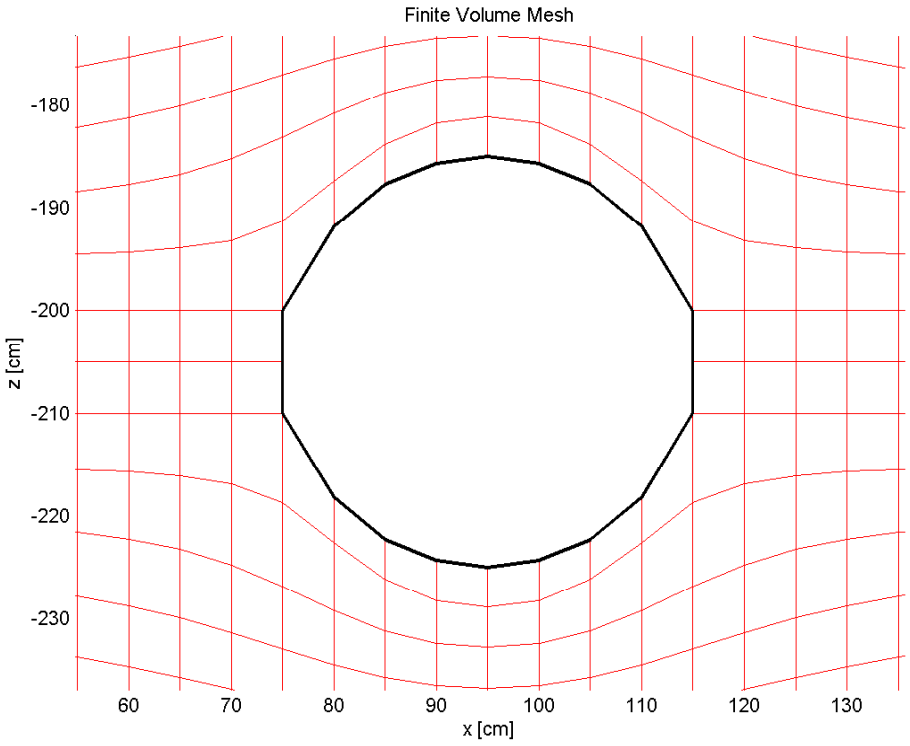

Figure 3.3: Close picture of grid near the drain pipe.

where $q_{ij'}$ is the size of the Darcy flux vector, perpendicular to the cell face and positive for flux out from cell i. The most easy way to implement Dirichlet boundary conditions is simply to force ψ_i to be value ψ has on face with Dirichlet conditions. Conflicts can arise if cell i have more than one face with Dirichlet condition. Instead, the Dirichlet boundary conditions is implemented as if the midpoint of the Dirichlet face was a neighbor cell. Similar to an interior cell face, a difussive and a gravitational contribution can be calculated:

$$B^D_{ij'}(\boldsymbol{\psi}) = D^D_{ij'}(\boldsymbol{\psi}) + G^D_{ij'}(\boldsymbol{\psi}) \tag{3.7}$$

where

$$D^D_{ij'}(\boldsymbol{\psi}) = |e_{ij'}|(\mathbf{K}(\psi_i) \cdot (\nabla\psi)_{ij'}) \cdot \bar{\mathbf{n}}_{ij'} \tag{3.8}$$

$$G^D_{ij'}(\boldsymbol{\psi}) = |e_{ij'}|(\mathbf{K}(\psi_i) \cdot ([0\ 1]^T)) \cdot \bar{\mathbf{n}}_{ij'} \tag{3.9}$$

where the pressure associated with cell i has been used for calculating the hydraulic conductivity.

The sink term can be divided into two parts

$$\Gamma = \Gamma_A + \delta(x_p - x)\delta(z_p - z) \tag{3.10}$$

where Γ_A is the contribution from area distributed sinks and Γ_P the contribution from point sinks. (x_p, z_p) is the coordinates of the point sink which NOT is placed on the faces of the cell. δ is the delta function of Dirac. Thus, the contribution from the sink term yield

$$S_i(\psi) = \Gamma_A|Q_i| + \Gamma_P \tag{3.11}$$

Area distributed sinks are typically extraction from roots or in Daisy2D water flow into or out from the macro pore domain. The point sinks can both be drains and from drip irrigation systems (point sources). Both Γ_A and Γ_P can in the prototype be dependent on the solution.

3.1.3 Rectangular cells

For the situation with a mesh consisting of rectangular cells, only matrix pressure in the four neighbor cells (se figure 3.4) are applied for calculating the fluxes through the faces of the cell (five point stencil). In the present section we will only evaluate the gradient for the "eastern" cell face of cell i. The theory can easily be applied for the 3 remaining directions.

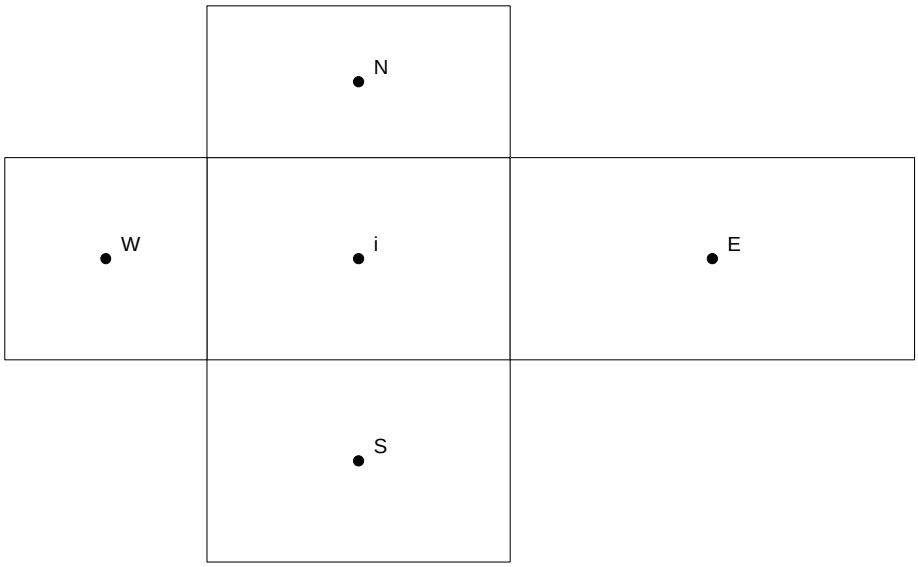

Figure 3.4: Cell i and the neighbor cells it share faces with.

The distances necessary for evaluating the flux from a cell to the cell placed east of the cell are shown in figure 3.5.

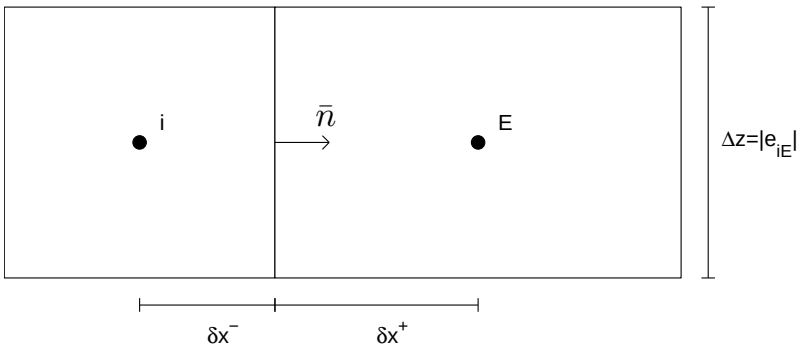

Figure 3.5: Distances used for calculation of flux between cell i and its "eastern" neighbor.

The value of ψ in the midpoint of the eastern cell (ψ_E) can be expressed by a Taylor expansion of the value of ψ at the midpoint of the cell face:

$$\psi_E = \psi(x + \delta x^+) = \sum_{k=0}^{m} \frac{1}{k!} \left(\frac{d^k \psi}{dx^k} \right)_f (\delta x^+)^k + R^+ \tag{3.12}$$

where m is the order of the Taylor expansion and R^+ is the Lagrange remainder. Similar can ψ_i be computed

$$\psi_i = \psi(x - \delta x^-) = \sum_{k=0}^{m} \frac{1}{k!} \left(\frac{d^k \psi}{dx^k} \right)_f (-\delta x^-)^k + R^- \tag{3.13}$$

It can be assumed that $R^+ - (-1)^{m+1} R^- \approx 0$. If a Taylor expansion of first order ($m = 1$) is chosen we get

$$\left(\frac{d\psi}{dx} \right)_f (\delta x^+ + \delta x^-) \approx \psi_E - \psi_i \tag{3.14}$$

If a higher order Taylor expansion is chosen we get

$$\left(\frac{d\psi}{dx} \right)_f (\delta x^+ + \delta x^-) \approx \psi_E - \psi_i - \epsilon_{Ei} \tag{3.15}$$

where the correction term can be calculated as

$$\epsilon_{Ei} \approx \sum_{k=2}^{m} \frac{1}{k!} \left(\frac{d^n \psi}{dx^n} \right)_f \left[(\delta x^+)^n - (-\delta x^-)^n \right] \tag{3.16}$$

It can be seen that a second order precision is obtained with $m = 1$ and $\delta x^+ = \delta x^-$. $m = 1$ is chosen for the relative simple model for rectangular cells.

The width and height of cell i are denoted $(\Delta x)_i$ and $(\Delta z)_i$ respectively, thus $\delta x^- = \frac{(\Delta x)_i}{2}$, $\delta x^+ = \frac{(\Delta x)_E}{2}$ and $|e_{iE}| = (\Delta z)_i = (\Delta z)_E$. The outwarded unit normal, $\bar{\mathbf{n}}_{iE} = [1\ 0]^T$. The diffusive transport through the cell eastern face is:

$$D_{iE}(\boldsymbol{\psi}) = (K_{xx})_{iE} \frac{2(\Delta z)_i}{(\Delta x)_E + (\Delta x)_i} (\phi_E - \phi_i) \tag{3.17}$$

The gravitational transport from cell i to cell E is:

$$G_{iE}(\boldsymbol{\psi}) = 0 \tag{3.18}$$

If the eastern cell face of cell i belongs to the boundary of Ω (no eastern neighbor), $B_{iE'}$ shall be calculated. If the cell face have a Neumann boundary condition we have

$$B^N_{iE'}(\boldsymbol{\psi}) = -q_{iE'}(\Delta z)_i \tag{3.19}$$

where $q_{iE'}$ is size of the flux transported out from through the cell face. If the cell face have a Dirichlet boundary condition:

$$D^D_{iE'}(\boldsymbol{\psi}) = (K_{xx})_i \frac{2(\Delta z)_i}{(\Delta x)_i} (\psi_{E'} - \psi_i) \tag{3.20}$$

where $\psi_{E'}$ is the value of ψ in the midpoint on the eastern cell face of cell i. The gravitational part gives:

$$G^D_{iE'}(\boldsymbol{\psi}) = 0 \tag{3.21}$$

3.1.4 Conductivity at cell faces

The conductivity at the cell faces between adjacent cells (as used in equations 3.3 and 3.4)are in Daisy calculated by either the arithmetic, logarithmic of harmonic mean. Physical arguments speaks for applying the harmonic mean:

$$\frac{1}{K_{ij}} = \frac{1}{2}\left[\frac{1}{K(\psi_i)} + \frac{1}{K(\psi_j)}\right] \tag{3.22}$$

3.1.5 Iteration scheme

By assembling 3.2 for $i = 1,\ 2\, cdots N$, the problem can be written as a ordinary differential equation (ODE) on the form:

$$\mathbf{Q}\frac{d\boldsymbol{\theta}}{dt} = \mathbf{E}(\boldsymbol{\psi})\boldsymbol{\psi} + \mathbf{F}(\boldsymbol{\psi}) \tag{3.23}$$

where $\mathbf{Q}$ is a diagonal matrix with $Q(i,i) = |Q_i|$ and $\theta = \theta(\psi)$. $\mathbf{E}(\boldsymbol{\psi})\boldsymbol{\psi}$ is the assembly of D_{ij} and $D^D_{ij'}$ and G_{ij}, $G^D_{ij'}$, $B^N_{ij'}$ and S_i is assembled in $\mathbf{F}(\boldsymbol{\psi})$. The equation is discretized in the time domain using the backward Euler method:

$$\mathbf{Q}\frac{\boldsymbol{\theta}^{n+1,m+1} - \boldsymbol{\theta}^n}{\Delta t} = \mathbf{E}(\boldsymbol{\psi}^{n+1,m})\boldsymbol{\psi}^{n+1,m} + \mathbf{F}(\boldsymbol{\psi}^{n+1,m}) \tag{3.24}$$

In order to get rid of θ at iteration step $m+1$, the mixed formulation by Celia *et al.* (1990) is applied. In the mixed formulation, the water content at time step $n+1$ and iteration step $m+1$ is approximated by a Taylor expansion:

$$\begin{aligned}\theta^{n+1,m+1} &= \theta^{n+1,m} + \frac{d\theta}{d\psi}\,|^{n+1,m}\,(\psi^{n+1,m+1} - \psi^{n+1,m}) \\ &= \theta^{n+1,m} + C^{n+1,m}(\psi^{n+1,m+1} - \psi^{n+1,m})\end{aligned} \tag{3.25}$$

where $C = \partial\theta/\partial\psi$ is the specific water capacity function. The time derivative of θ can then be approximated as:

$$\begin{aligned}\frac{\partial\theta}{\partial t} &\approx \frac{\theta^{n+1,m+1} - \theta_n}{\Delta t} = \frac{\theta^{n+1,m+1} - \theta^{n+1,m}}{\Delta t} + \frac{\theta^{n+1,m} - \theta_n}{\Delta t} \\ &\approx C^{n+1,m}\frac{\psi^{n+1,m+1} - \psi^{n+1,m}}{\Delta t} + \frac{\theta^{n+1,m} - \theta^n}{\Delta t}\end{aligned} \tag{3.26}$$

Thus, the iterative scheme is

$$\left(\frac{1}{\Delta t}\mathbf{QC}(\boldsymbol{\psi}^{n+1,m}) - \mathbf{E}(\boldsymbol{\psi}^{n+1,m})\right)\boldsymbol{\psi}^{n+1,m+1} =$$
$$\mathbf{F}(\boldsymbol{\psi}^{n+1,m}) + \frac{1}{\Delta t}\mathbf{QC}(\boldsymbol{\psi}^{n+1,m})\boldsymbol{\psi}^{n+1,m} + \frac{1}{\Delta t}\mathbf{Q}\left(\boldsymbol{\theta}^{n} - \boldsymbol{\theta}^{n+1,m}\right) \tag{3.27}$$

where $\mathbf{C}$ is a diagonal matrix with $C(i,i) = C_i$.

In the MATLAB-prototype it is possible to chose simulations with a constant or dynamically size of the time steps, Δt. For the last choice, the size of Δt depends on how difficult it is to obtain a solution. A procedure based on same principles is described in Mollerup (2001). In Daisy2D other processes than matrix flow shall be taken into account, and the time stepping routine will be changed.

3.1.6 Matrix solution technique

In the prototype, for solving the large matrix system of the type $\mathbf{Ax} = \mathbf{b}$ (see equation 3.27), the MATLAB backslash operator (also called leftdivision) is used. For description of the applied sparse matrix solver is refereed to Mollerup (2001).

3.1.7 Hydraulic properties

In the Daisy2D it shall be possible to chose between the existing models for the soil hydraulic properties in Daisy. In the prototype, the retention characteristics described with the model by van Genuchten (1980):

$$\begin{aligned} \theta = \theta_r + \frac{\theta_s - \theta_r}{[1 + |\alpha\psi|^n]^m} \qquad & \text{for } \psi < 0 \\ \theta = \theta_s \qquad & \text{for } \psi \geq 0 \end{aligned} \tag{3.28}$$

where α, n and m are empirical parameters, θ_s and θ_r are the saturated and the residual water content, respectively. By combination with the hydraulic conductivity model by Mualem (1976) and choosing $m = 1 - 1/n$, the hydraulic conductivity can be calculated as

$$K = K_s S_e^{1/2}[1 - (1 - S_e^{1/m})^m]^2 \tag{3.29}$$

where K_s is the hydraulic conductivity at saturation and S_e is the effective saturation defined as

$$S_e = \frac{\theta - \theta_r}{\theta_s - \theta_r} \tag{3.30}$$

The retention model by van Genuchten have been adopted to a large class of soils.

3.2 Verification

The FVM-code i verified by comparing solutions obtained by FVM with quasi-analytical solutions for one-dimensional infiltration by Philip.

3.2.1 Infiltration Model of Philip

Philip (1957b) showed that the infiltration depth as function of time and saturation can be written as a power series in $t^{\frac{1}{2}}$. The coefficients are then functions of soil water content, θ. From the expression for the infiltration depth, as function of water content and time. It is then relatively easy to derive that the cumulative infiltration, also can be written as a power series in $t^{\frac{1}{2}}$. The assumptions for the theory is an 1-dimensional vertical flow into a homogenous soil semi-infinite soil column, initially with uniform water content. The cumulative infiltration is expressed as

$$I = \sum_{n=1}^{+\infty} A_n t^{\frac{n}{2}} \tag{3.31}$$

where $A_1 = S$ is the often refereed sorptivity as defined in Philip (1969). The coefficients are found by solving a set of successive integro-differential equations. One drawback of the power series theory is that the theory only describes the infiltration process well for short to intermediate times. The power series is "practical convergent" for $t < t_{\text{grav}}$. Where t_{grav} is the characteristic time of the infiltration process

$$t_{\text{grav}} = \left(\frac{S}{K_0 - K_i} \right)^2 \tag{3.32}$$

where $K_i = K(\theta_i)$ and $K_0 = K(\theta_0)$ is the hydraulic conductivity corresponding to the initial water content, θ_i and the water content at the soil surface, θ_0. For ponded conditions at the soil surface is $K_0 = K_s$.

The soil parametrization, which is applied for the comparative study, is the G.E. silt loam (van Genuchten 1980) where $K_s = 4.96$ cm/day, $\theta_s = 0.396$ cm^3/cm^3, $\theta_r = 0.131$ cm^3/cm^3, $\alpha = 0.00423$ cm^{-1} and $n = 2.06$.

In the verification simulations, a constant size of the time steps in the FVM simulations, Δt= 1/60 day has been applied. For all simulations the initial condition is h_i=-200 cm, corresponding to $\theta_i = 0.332$ cm^3/cm^3 chosen.

Vertical falling-head infiltration

Initially, it was shown that the power series solution can be applied for non-saturated or just saturated conditions at the soil surface (see Philip 1955, 1957b,a). Philip (1958) later expanded the theory to cover also ponding situations with constant positive pressure at the soil surface. Later it was shown

(Mollerup 200x) that the power series solution also can be applied for a falling-head condition, where the ponding depth is dependent on the amount of infiltrated water. The pressure at the soil surface is then

$$H = H_0 - I \tag{3.33}$$

where H_0=20 cm is the initial ponding depth.

In the FVM simulations, both the vertical and horizontal discretisation, $\Delta z = \Delta x$ is 1 cm. The lower boundary was placed at $z = 600$ cm with a free drainage (gravity flow) condition. For the scenario is t_{grav}=3.34 days and the time at which the pond empties, t_p =2.6022 days is computed by applying the iteration procedure as proposed in Mollerup (200x). In FVM-simulation, the pond empties at approximately t =2.5833 days. I.e. t_p is approximately 0.7% higher for the power series solution than for the similar FVM results obtained with a rather rough time discretisation. Minor errors can be expected in the power series solution as only the first 4 terms are calculated. For constant-head simulation the first 6 terms are calculated. Philip (1957b) found that normally only first two or three terms are necessary for a for practical use sufficient correct solutions.

In Figure 3.6, the wetting profiles as calculated by applying FVM and the power series theory are shown. The wetting profiles are shown for t = 1/5, 2/5, 3/5, 4/5 and $1 \cdot t_{\text{p}}$. As it can be observed, the solutions are almost identical except for $t = t_{\text{p}}$ (2.6022 days) where the effects of the slightly earlier emptying ponded water in the FVM simulation instantly effects the water content profiles.

3.2.2 Horizontal constant-head infiltration

For also insuring that horizontal are simulated correctly a simulation with a horizontal column is made. For the FVM simulation, the column is has height of 1 cell and a width of 800 cells with $\Delta x = \Delta z$ =1 cm. The left boundary condition is H =20 cm and the initial condition is h_n =-200 cm. Vertical constant-head infiltration can analytically be calculated as:

$$I = A_1 \sqrt{(t)} \tag{3.34}$$

Where A_1 is identical to the A_1 calculated for vertical infiltration with constant-head (and falling-head) conditions. Contrary to vertical infiltration, equation 3.34 is applicable also for large times. Figure 3.7 shows the water content profiles at t = 1/5, 2/5, 3/5, 4/5 and $1 \cdot t_{\text{grav}}$. as calculated with FVM and the power series theory. As it can be seen are the solutions almost identical.

3.2.3 Vertical constant-head infiltration in a wide column

Until now the all the verifications simulations are all made meshed with a length of 1 cell in the direction perpendicular to the flow direction. Also the size of the

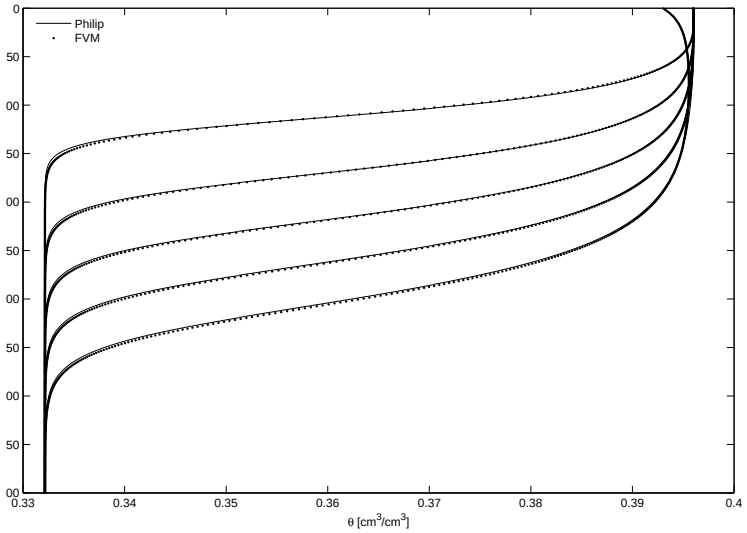

Figure 3.6: Analytical and FVM solution for vertical falling head infiltration. The solution is shown for $t = 1/5,\ 2/5,\ 3/5,\ 4/5$ and $1 \cdot t_{\mathrm{p}}$.

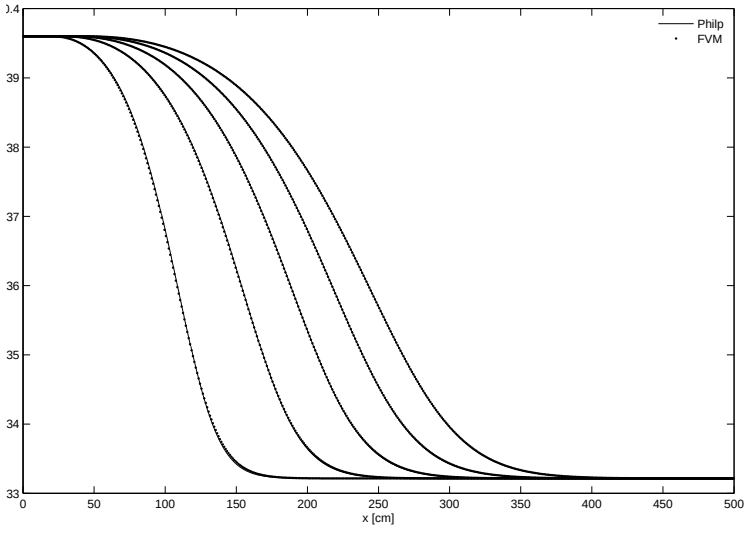

Figure 3.7: Analytical and FVM solution for horizontal infiltration. The solution is shown for $t = 1/5,\ 2/5,\ 3/5,\ 4/5$ and $1 \cdot t_{\mathrm{grav}}$.

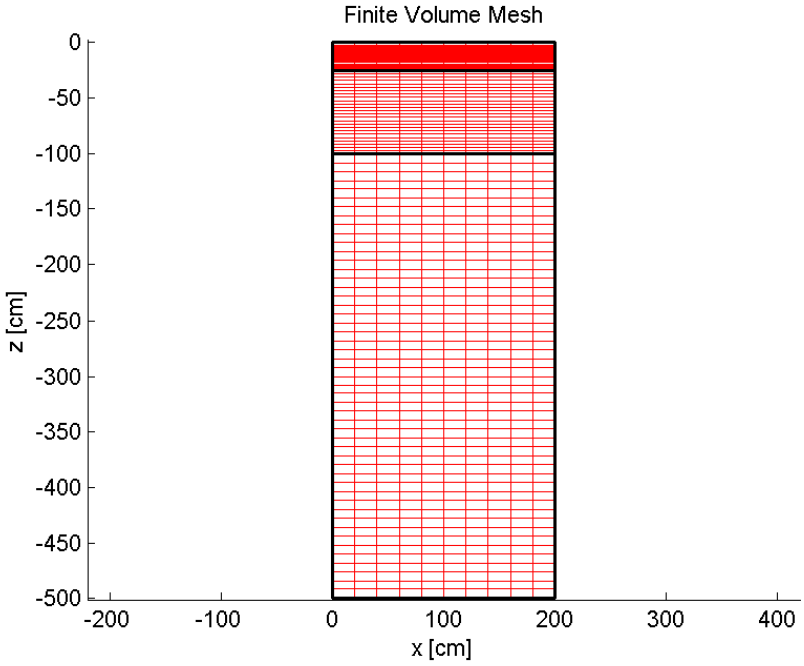

Figure 3.8: Mesh for the wide column simulation.

cells where equal. In the wide column experiment the cell height varies with the depth. The soil column consists of 3 horizons (A, B and C). The A-horizon is 25 cm depth with Δz =1 cm, the B-horizon is 75 cm depth with Δz =3 cm, and the C-horizon is 400 cm depth with Δz =8 cm. The soil column have a width of 200 cm with Δx =20 cm. Figure 3.8 shows the mesh and figure 3.9 shows a upper part of the mesh.

In the simulation is the ponding depth constantly $H = 20$ cm. Figure 3.10 shows the water content after 1 day. As it can be observed, the water do not variate with the x-coordinate for a given depth, i.e. there is no indication of unintended exchange of water between internal vertical cell boundaries.

Also here (not shown) comparisons with a power series solution shown fine agreement

3.2.4 Other simulations

There have also been made simulations with a Neumann (flux) condition at the soil surface. Also simulations with a non zero sink term has been conducted. All the simulations showed excellent mass-balances.

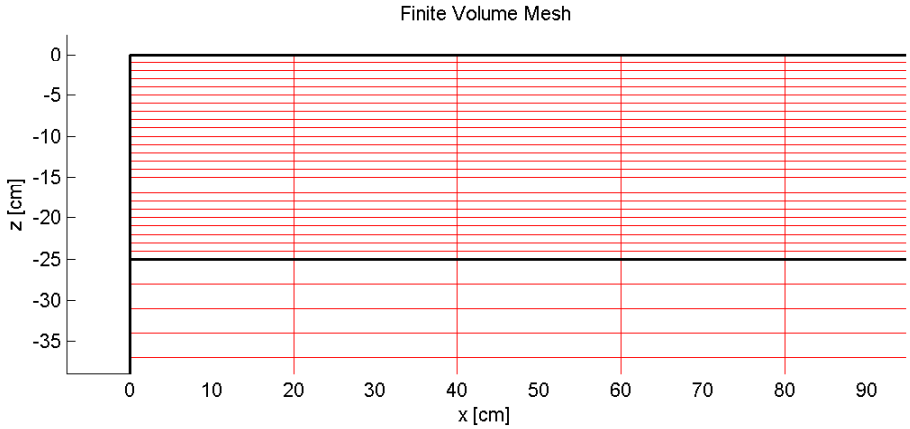

Figure 3.9: Upper left part of mesh used for the wide column simulation.

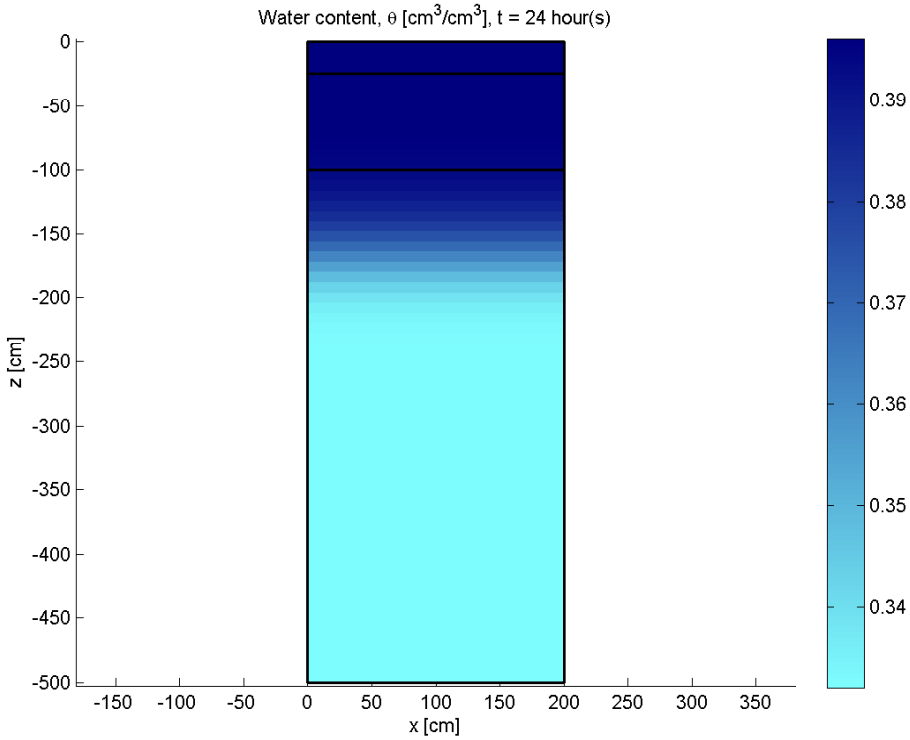

Figure 3.10: Water distribution after 1 day in the wide column simulation.

Bibliography

Celia, M. A., Bouloutas, E. T., og Zarba, R. L. (1990). A general mass-conservative numerical solution for the unsaturated flow equation. *Water Resour. Res.*, **26**(7), 1483–1496.

Mollerup, M. (2001). *Numerical Modelling of Water and Solute Movement in Tilled Topsoil*. Ph.D. thesis, The Royal Veterinary and Agricultural University, Tåstrup, Denmark.

Mollerup, M. (200x). Power series solution for falling-head ponded infiltration. *Water Resour. Res.*, **xx**, xxxx–xxxx. Accepted with minor revisions.

Mualem, Y. (1976). A new model for predicting the hydraulic conductivity of unsaturated porous media. *Water Resour. Res.*, **12**(3), 513–522.

Philip, J. R. (1955). Numerical solution of equations of the diffusion type with diffusivity concentration-dependent. *Transaction of the Faraday Society*, **51**(7), 885–892.

Philip, J. R. (1957a). Numerical solution of equations of the diffusion type with diffusivity concentration-dependent. II. *Australian Journal of Physics*, **10**, 29–42.

Philip, J. R. (1957b). The theory of infiltration: 1. the infiltration equation and its solution. *Soil Sci.*, **83**, 345–357.

Philip, J. R. (1958). The theory of infiltration: 6. effect of water depth over soil. *Soil Sci.*, **85**, 278–286.

Philip, J. R. (1969). Theory of infiltration. *Advances in hydroscience*, pages 215–296.

van Genuchten, M. T. (1980). A closed-form equation for predicting the hydraulic conductivity of unsaturated soils. *Soil Sci.*, **44**.